Dynamics of Star Polymers branch point motion

Laurence Hawke

Daniel Read

Petra Bačová

Angel Moreno

Melt state

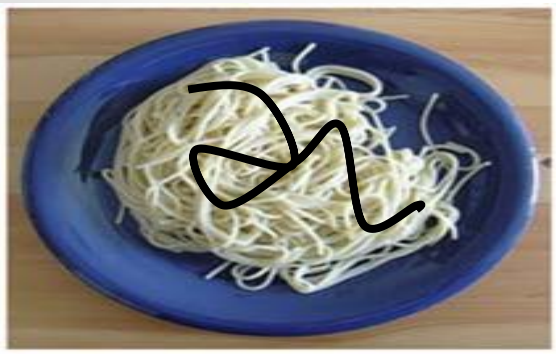

Tube models

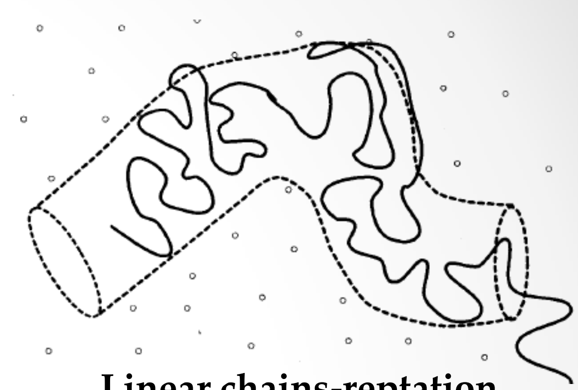

Linear chains-reptation

M. Doi and S.F. Edwards, "The Theory of Polymer Dynamics", Oxford University Press, Oxford, (1986)

commercial polymers are usually highly and randomly branched e.g. LDPE

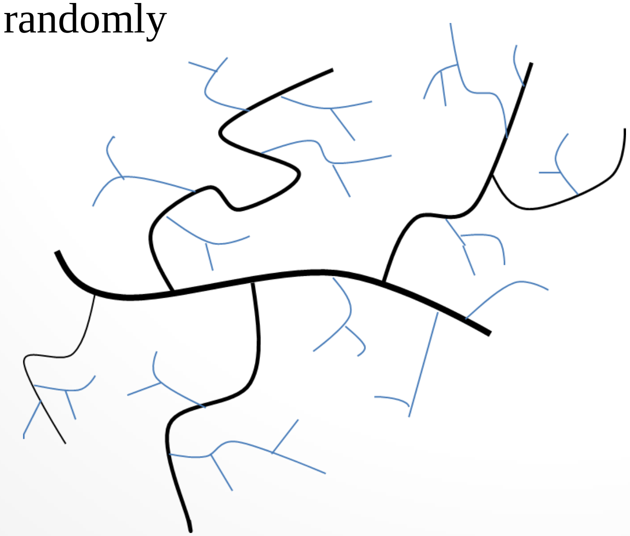

Rheological properties of linear/branched polymers:

Similar behaviour under shear flow: *Shear thinning*

Dramatically different behaviour under extensional flow

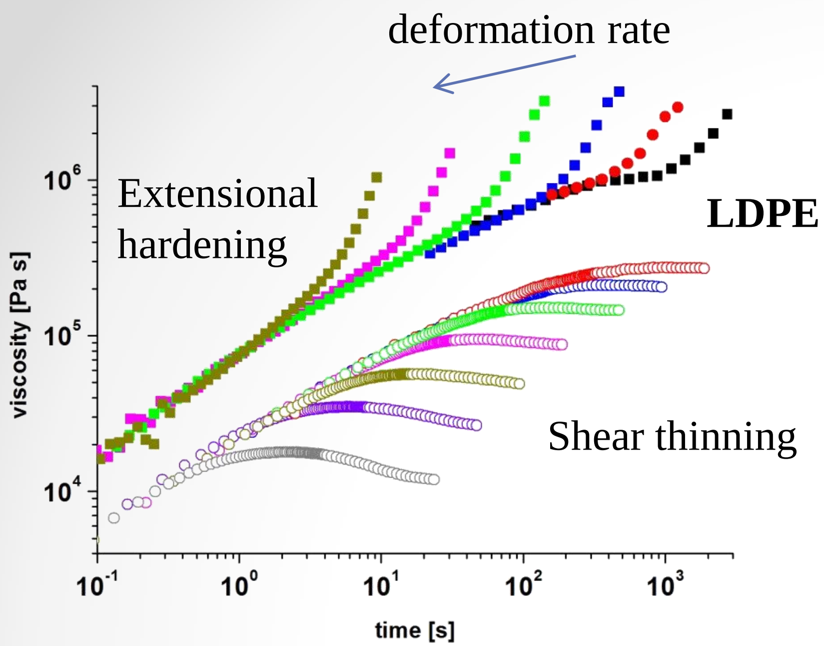

Extensional hardening is desirable in processing flows dominated by extensional flows / film blowing

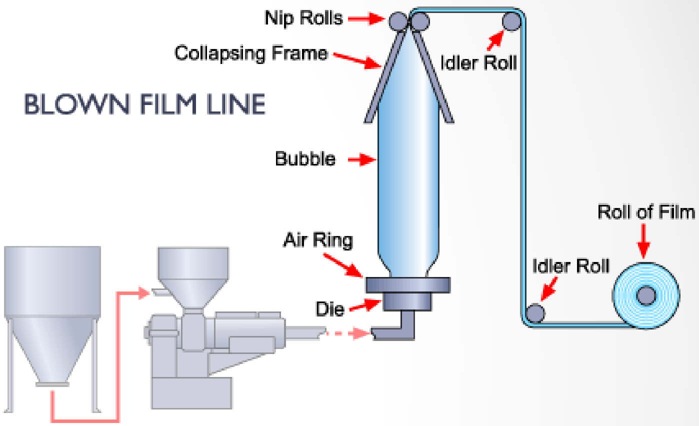

Why LDPEs exhibit extensional hardening?

T.C.B. Mc Leish and R.G. Larson, J. Rheology 42, 81, (1998)

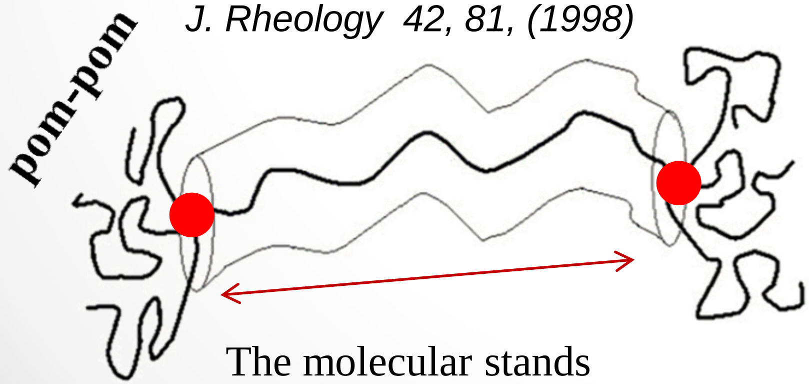

The molecular stands that lie between branch points stretch and produce the extensional hardening

Local motion of branch points

Relaxation of star polymers

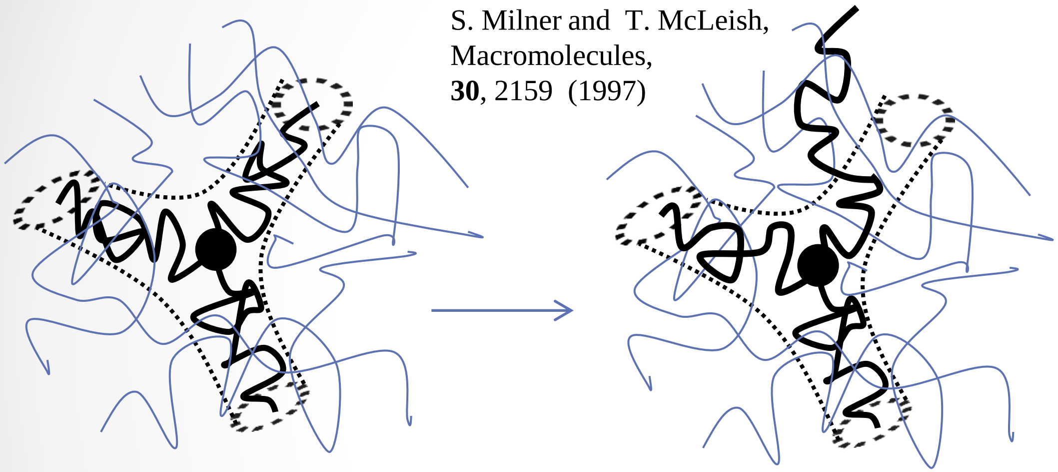

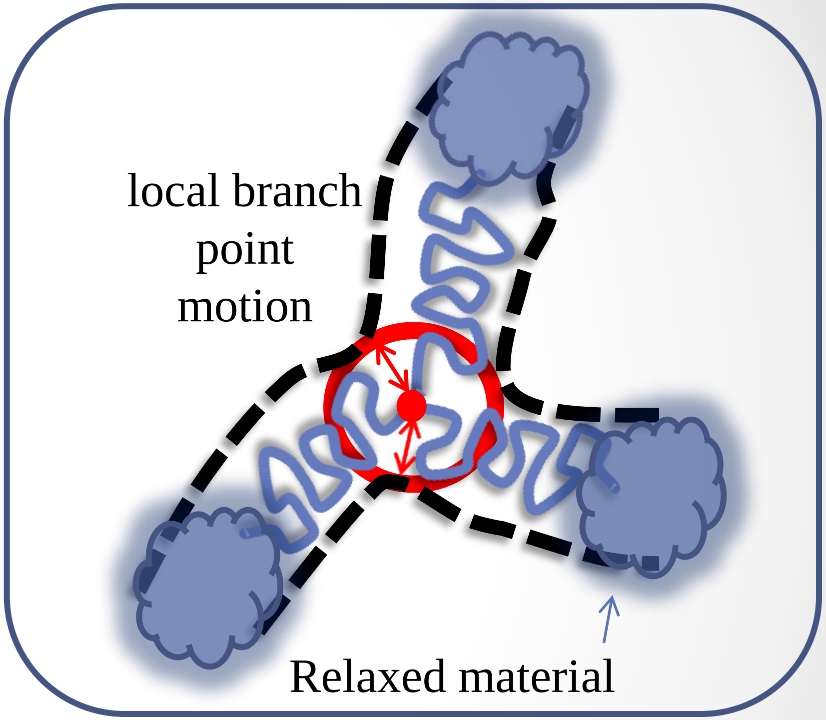

Reptation is entropically unfavourable- relaxation occurs via thermally activated retractions

Develop an expression for the MSD of the branch point and compare it with MD data

THEORY

Rouse model-unentangled linear chains

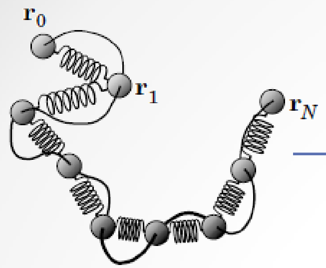

$$\zeta \frac{\partial \mathrm{R}_n(t)}{\partial t} = k \frac{\partial^2 \mathrm{R}_n(t)}{\partial n^2} + \mathrm{f}_n$$

Rouse, P.E., J. Chem. Phys. **21**, 1272 (1953)

$$\mathrm{X}_p(t) = \frac{1}{N} \int_0^N \mathrm{R}_n(t) \cos\left(\frac{p\pi n}{N}\right) dn$$

$$\boxed{\mathrm{R}_n(t) = \mathrm{X}_0(t) + 2 \sum_{p=1}^{\infty} \mathrm{X}_p(t) \cos\left(\frac{p\pi n}{N}\right)}$$

Split the chain into N/p domains (modes)

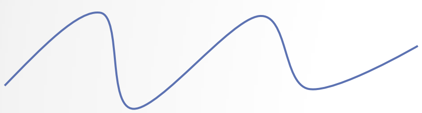

p=1

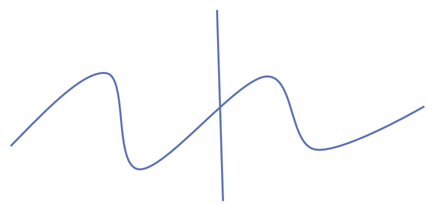

p=2

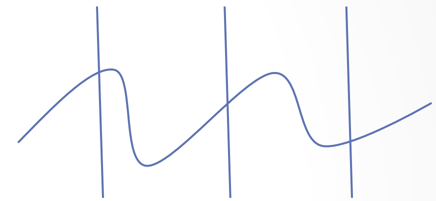

p=4

…etc

Fast modes (high p)-The conformation of the chain changes locally

Slow modes (low p) - the conformation of the chain changes globally

$$\tau_p = \frac{\tau_R}{p^2}$$

$$\tau_R = \frac{\zeta b^2 N^2}{3\pi^2 k_B T}$$

THEORY

Dynamics of Unentangled Stars

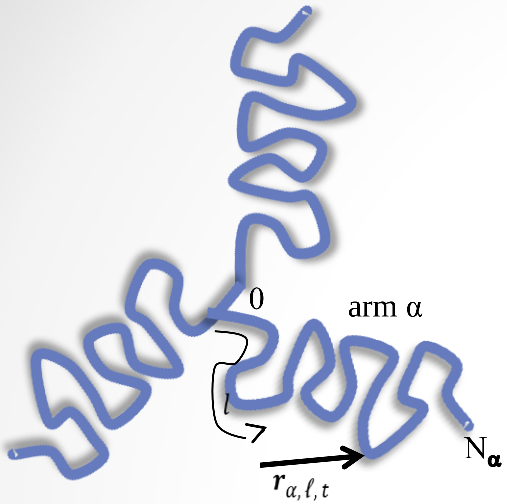

Rouse equation $$\zeta \frac{\partial}{\partial t}\boldsymbol{r}_{\alpha,\ell,t} = k\frac{\partial^2}{\partial \ell^2}\boldsymbol{r}_{\alpha,\ell,t} + \boldsymbol{g}$$

Appropriate boundary conditions

1. Chain connectivity at the branchpoint.
2. Force balance at the branchpoint.
3. No force at the chain ends.

$$\boldsymbol{r}_{\alpha,\ell,t} = \sum_p \boldsymbol{X}_p^c(t)\Phi_p^c(\ell) + \sum_q [\boldsymbol{X}_q^{s1}(t)\Phi_q^{s1}(a,\ell) + \cdots + \boldsymbol{X}_q^{s_f{}'}(t)\Phi_q^{s_f{}'}(a,\ell)]$$

$\boldsymbol{X}_p^c(t), \boldsymbol{X}_q^{s_i}(t)$ the time dependent eigenmode amplitudes

$$\Phi_p^c(\ell) = \cos\left(\frac{p\pi\ell}{N_a}\right)$$ cosine eigenmodes of degeneracy 1

$$\Phi_q^{s_i}(a,\ell) = s_{ia}\sin\left(\frac{(2q-1)\pi\ell}{2N_a}\right)$$ sine eigenmodes of degeneracy *f*-1

THEORY

Dynamics of Entangled Stars

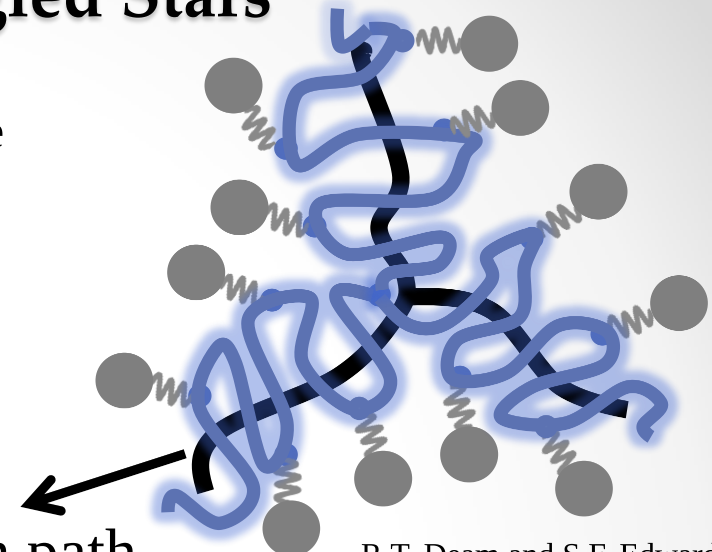

Entanglements are modelled by localising each Rouse segment in its own harmonic potential

Effect of localising spring: each segment fluctuates about an averaged position (averaged over τ_e)

D.J. Read,
K. Jagannathan,
and A.E. Likhtman
Macromolecules,
41, 6843 (2008).

$$\boldsymbol{r}_{\alpha,\ell,t} = \bar{\boldsymbol{r}}_{\alpha,\ell} + \boldsymbol{\Delta}_{\alpha,\ell,t}$$

R.T. Deam and S.F. Edwards
Phil. Trans. Roy. Soc. London Ser. A, **280,** 317 (1976)

$$\boldsymbol{\Delta}_{\alpha,\ell,t} = \sum_p \boldsymbol{\Upsilon}_p^c(t)\Phi_p^c(\ell) + \sum_q [\boldsymbol{\Upsilon}_q^{s1}(t)\Phi_q^{s1}(a,\ell) + \cdots + \boldsymbol{\Upsilon}_q^{s_f{}'}(t)\Phi_q^{s_f{}'}(a,\ell)]$$

$$\zeta \frac{\partial}{\partial t}\boldsymbol{\Delta}_{\alpha,\ell,t} = k\frac{\partial^2}{\partial \ell^2}\boldsymbol{\Delta}_{\alpha,\ell,t} - kh_s\boldsymbol{\Delta}_{\alpha,\ell,t} + \boldsymbol{g}$$

Fast modes (high p) →fluctuations within the tube

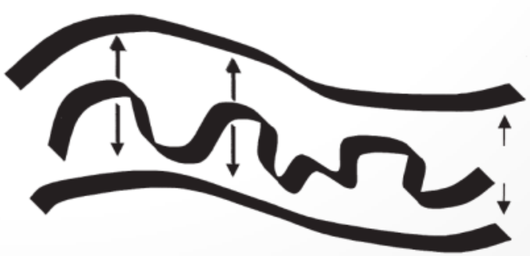

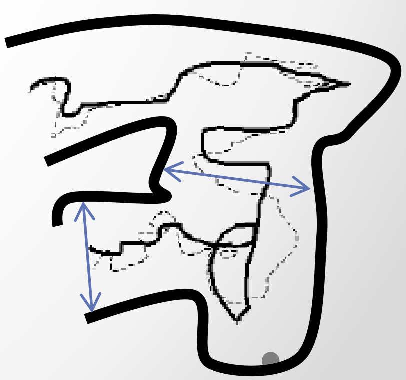

	Unentangled	Entangled
MSD of two different beads **same arm**	$\frac{2b^2}{\pi^{1.5}}\sqrt{\tilde{\tau}}\,e^{\frac{-\pi^2\lvert\ell-\ell'\rvert^2}{4\tilde{\tau}}} + \lvert\ell-\ell'\rvert b^2\Phi\left(\frac{\pi\lvert\ell-\ell'\rvert}{2\sqrt{\tilde{\tau}}}\right) - \left(\frac{f-2}{f}\right)\frac{2b^2}{\pi^{1.5}}\sqrt{\tilde{\tau}}\,e^{\frac{-\pi^2(\ell+\ell')^2}{4\tilde{\tau}}} - \left(\frac{f-2}{f}\right)(\ell+\ell')b^2\left[\Phi\left(\frac{\pi(\ell+\ell')}{2\sqrt{\tilde{\tau}}}\right)-1\right]$	$\lvert s-s'\rvert d^2 + \frac{d^2}{2}e^{-2\lvert s-s'\rvert} - \frac{d^2}{2}\left(\frac{f-2}{f}\right)e^{-2(s+s')} - \frac{d^2}{4}\left[2cosh[2\lvert s-s'\rvert] - e^{-2\lvert s-s'\rvert}\,\Phi\left(\frac{2\sqrt{\tilde{\tau}}}{\pi}-\frac{\pi\lvert s-s'\rvert}{2\sqrt{\tilde{\tau}}}\right) - e^{2\lvert s-s'\rvert}\Phi\left(\frac{2\sqrt{\tilde{\tau}}}{\pi}+\frac{\pi\lvert s-s'\rvert}{2\sqrt{\tilde{\tau}}}\right)\right] + \frac{(f-2)d^2}{4f}\left[2cosh[2(s+s')] - e^{-2(s+s')}\,\Phi\left(\frac{2\sqrt{\tilde{\tau}}}{\pi}-\frac{\pi(s+s')}{2\sqrt{\tilde{\tau}}}\right) - e^{2(s+s')}\Phi\left(\frac{2\sqrt{\tilde{\tau}}}{\pi}+\frac{\pi(s+s')}{2\sqrt{\tilde{\tau}}}\right)\right]$
MSD of two different beads **different arms**	$\frac{(\ell+\ell')b^2}{f}\left[(f-2)+2\Phi\left(\frac{\pi(\ell+\ell')}{2\sqrt{\tilde{\tau}}}\right)\right] + \frac{4b^2}{f\pi^{1.5}}\sqrt{\tilde{\tau}}\,e^{\frac{-\pi^2(\ell+\ell')^2}{4\tilde{\tau}}}$	$(s+s')d^2 + \frac{d^2}{f}e^{-2(s+s')} - \frac{d^2}{f}cosh[2(s+s')] + \frac{d^2}{2f}\left[e^{-2(s+s')}\Phi\left(\frac{2\sqrt{\tilde{\tau}}}{\pi}-\frac{\pi(s+s')}{2\sqrt{\tilde{\tau}}}\right) + e^{2(s+s')}\Phi\left(\frac{2\sqrt{\tilde{\tau}}}{\pi}+\frac{\pi(s+s')}{2\sqrt{\tilde{\tau}}}\right)\right]$
Segmental motion	$2b^2\ell\left(\frac{f-2}{f}\right)\left[1-\Phi\left(\frac{\pi\ell}{\sqrt{\tilde{\tau}}}\right)\right] + \frac{2b^2}{\pi^{1.5}}\sqrt{\tilde{\tau}}\left[1-\left(\frac{f-2}{f}\right)e^{-\frac{\pi^2\ell^2}{\tilde{\tau}}}\right]$	$\frac{d^2}{2}\Phi\left(\frac{2\sqrt{\tilde{\tau}}}{\pi}\right) - \frac{d^2}{4}\left(\frac{f-2}{f}\right)e^{-4s}\left[1+\Phi\left(\frac{2\sqrt{\tilde{\tau}}}{\pi}-\frac{\pi s}{\sqrt{\tilde{\tau}}}\right)\right] + \frac{d^2}{4}\left(\frac{f-2}{f}\right)e^{4s}\left[1-\Phi\left(\frac{2\sqrt{\tilde{\tau}}}{\pi}+\frac{\pi s}{\sqrt{\tilde{\tau}}}\right)\right]$
branch point	$\frac{2}{f}\frac{2b^2}{\pi^{1.5}}\sqrt{\tilde{\tau}}$	$\frac{d^2}{f}\Phi\left(\frac{2\sqrt{\tilde{\tau}}}{\pi}\right)$

Compare with the MD Simulations

Fit Neutron Spin Echo Data

M. Zamponi et al., Macromolecules, ***43****, 518 (2010).*

THEORY

Interpetation of the expressions

- at equilibrium reduce to the Gaussian chain result

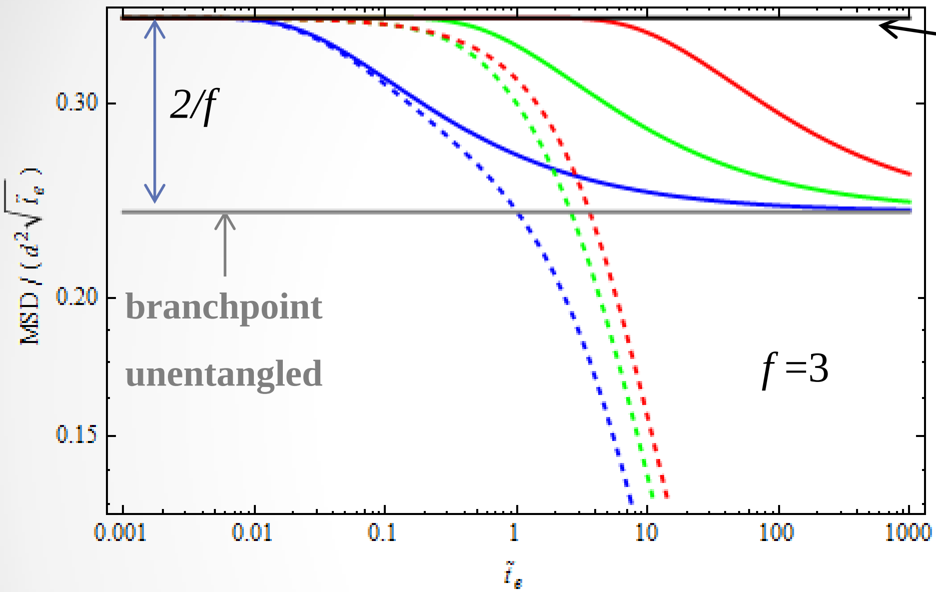

segmental motion

unentangled

linear chain

center

$s_1 < s_2 < s_3$

bp $\longrightarrow$

from chain to tube coordinates

$$s = \frac{\ell}{N_e} \quad a^2 = N_e b^2$$

$$\check{t}_{R_a} = \check{t}_e \left(\frac{N_e}{N_a}\right)^2$$

- At very early timescales all segments follow the segmental behaviour of an unentangled linear chain
- Segments closer to the branchpoint depart earlier from this kind of behaviour since they carry extra friction
- The plateau value decreases for segments closer to the branchpoint

COMPARISON

Fixed ends

Cayley tree

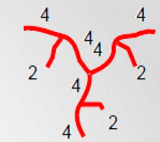

Systems: 3 arm stars with 8 entanglements per arm (888) and Cayley tree.

arm ends are fixed → **CR quenched**

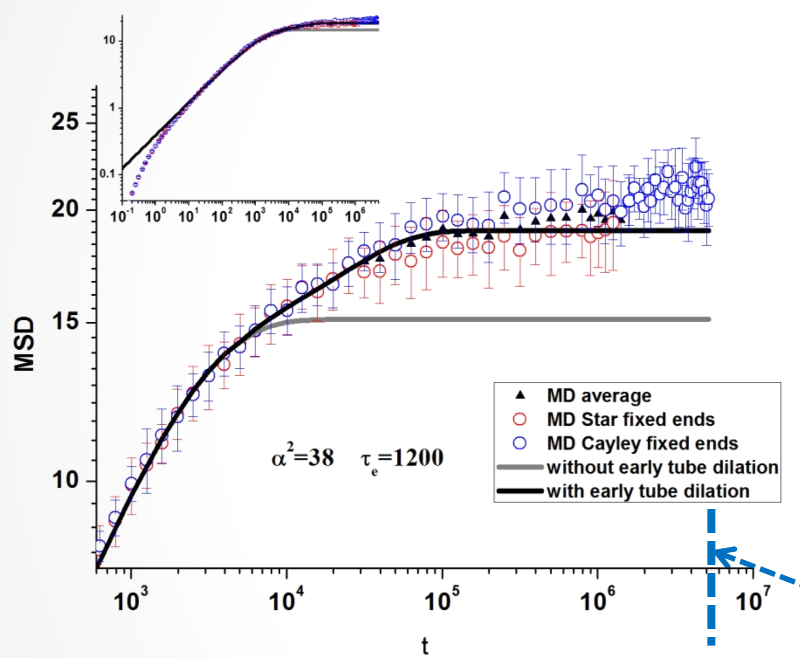

The **theory** goes through **a clear plateau** but **not the MD data**

We assume that the tube dilation process depends on time **weakly** so we rescale the model parameters:

$$d^2(t) = \frac{{d_0}^2}{g(t)}, \tau_e = \frac{\tau_{e0}}{g^2(t)}, s(t) = s_0 g(t)$$

$$g(t) = A + Be^{-\frac{t}{D}}$$

15% increase in tube diameter

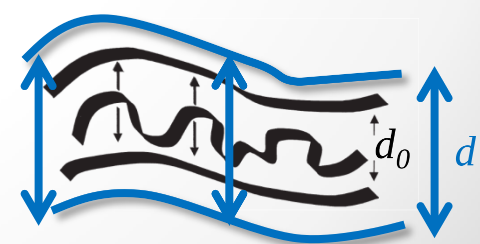

Explanation?

- excursions along the tube of each arm
- tension equilibration along the chains

COMPARISON

Free ends 1 – CR is now active

We need to know the tube survival probability $\phi(t)$. This can be obtained

A. From the **MD trajectories (without a mean path analysis):** From the time correlation function of the **tangent vectors** at two different segments.

P. S. Stephanou et al., J. Chem. Phys., **132**, 124904 (2010)

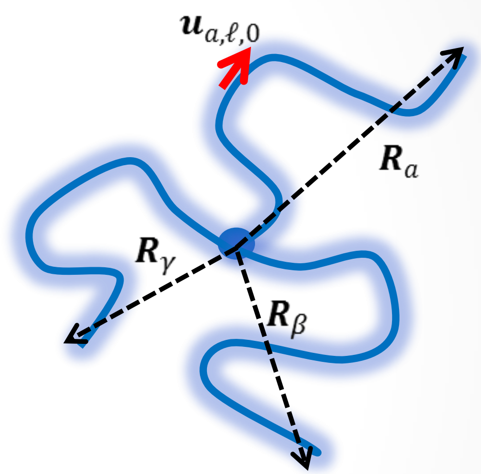

.

$$\psi_\ell(t) =< \boldsymbol{u}_{a,\ell,0} \cdot (\boldsymbol{R}_a - A\boldsymbol{R}_\beta - B\boldsymbol{R}_\gamma) >$$

$\boldsymbol{u}_{a,\ell,0}$: a bond vector at $t=0$

$\boldsymbol{R}_a$: end to end vector at t

B. From **BOB** (a free software that calculates the rheology of polymer melts of arbitrary architecture)

http://sourceforge.net/projects/bob-rheology

C. Das, N.J. Inkson, D.J. Read, and M.A. Kelmanson, The Journal of Rhology, **50**, 207 (2006)

In either case the model parameters are rescaled as:

$$d^2 = \frac{d_0^2}{g(t)\varphi(t)^a}\ ,\ \tau_e = \frac{\tau_{e0}}{g(t)^2\varphi(t)^{2a}}\ ,\ s(t) = s_0 g(t)\varphi(t)^a$$

Free ends 2 – Entangled case/MD data

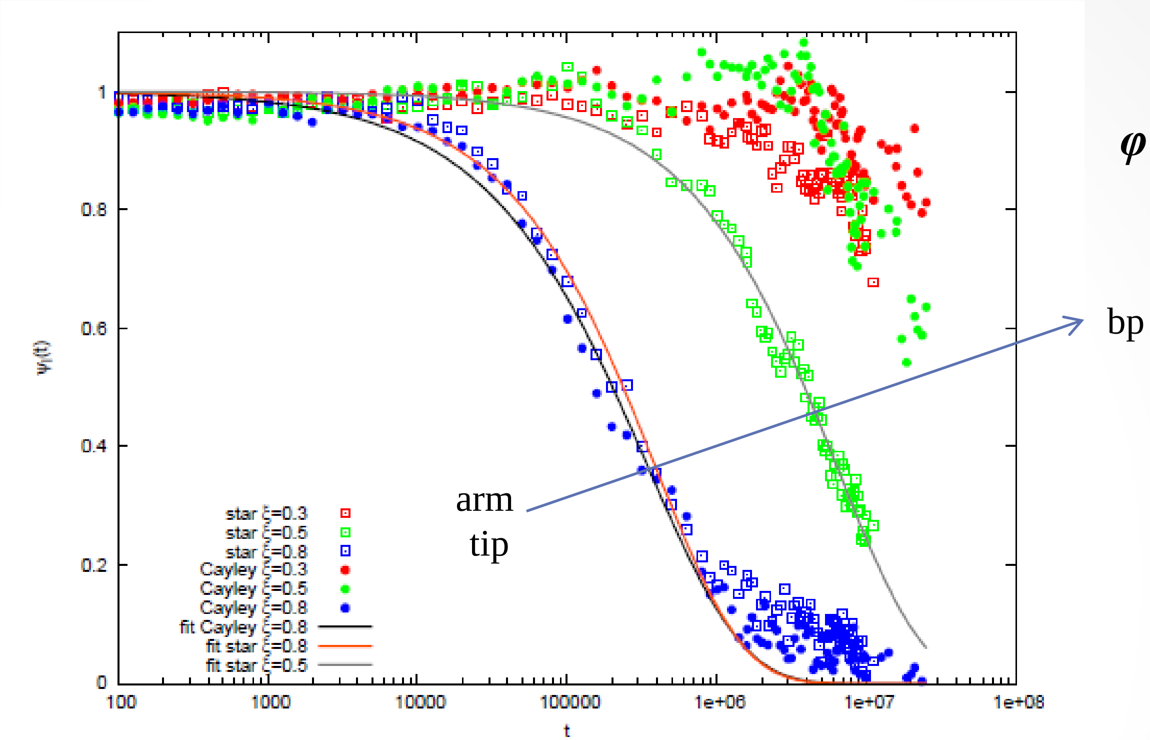

***φ(t) from* MD 2**

Fit the data with a stretched exponential function $\psi_\ell(t) = Ce^{-\left(\frac{t}{\tau_\ell}\right)^c}$

to obtain the relaxation spectrum of the arm $[\ell, \tau_\ell] \Rightarrow x(t)$

$$\varphi(t) = \frac{Z_\alpha[1 - \mathrm{x}_\alpha(t)] + Z_\beta[1 - \mathrm{x}_\beta(t)] + Z_\gamma[1 - \mathrm{x}_\gamma(t)]}{Z_\alpha + Z_\beta + Z_\gamma}$$

COMPARISON

Free ends 3

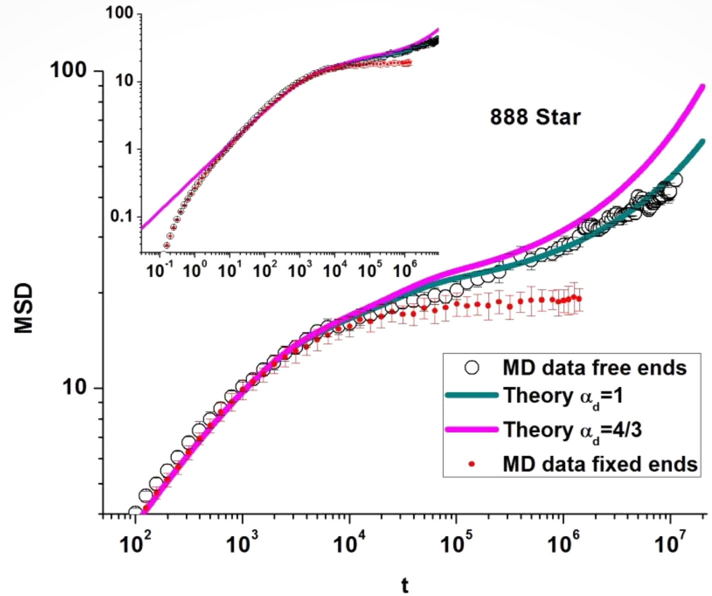

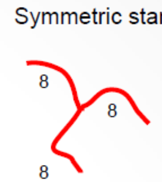

The agreement shows that φ(t) describes well the loss of confinement of the bp

Overall there is a good agreement between MD data and theory for α_d=1

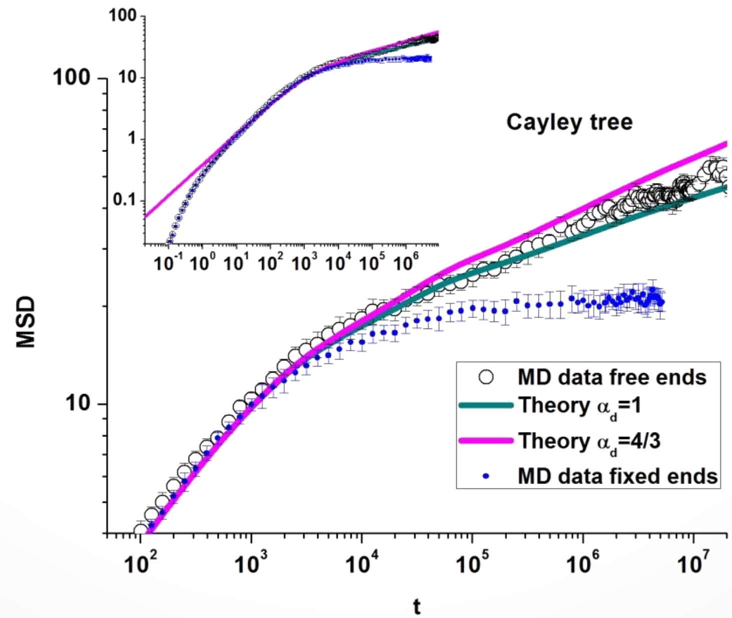

Verification of the dynamic dilution hypothesis

T.C.B. McLeish, Adv. Phys., **51**, 1379 (2002)

Conclusions

I. We have used the WE picture of the tube to develop expressions for the MSD of segments in the vicinity of branchpoints

II. Tube dilation is going on even if arm ends are fixed.

III. We have shown that one can "measure" $\varphi(t)$ from the MD simulations

IV. This gives a good prediction for the loss of confinement of the branchpoint and verifies the dynamic dilution hypothesis

MARIE CURIE ACTIONS

Dynamics of Architecturally Complex Polymers dynacop

UNIVERSITY OF LEEDS

https://eudoxus.leeds.ac.uk/dynacop/

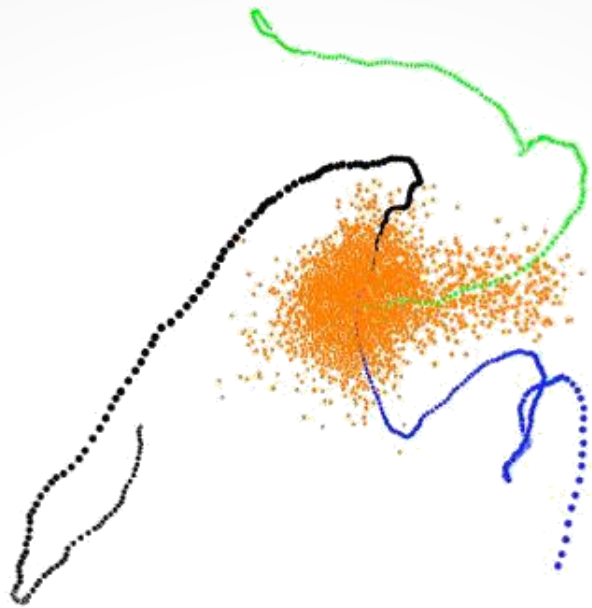

Figure 9: For a selected star in the simulations with fixed ends, trajectory of the branch point (orange dots) and mean paths of the three arms (black, blue and green). Perspective depth is used. A deep fluctuation of the branch point along the green arm is clearly observed.

$$\zeta \frac{\partial}{\partial t}\boldsymbol{\Delta}_{\alpha,\ell,t} = k\frac{\partial^2}{\partial \ell^2}\boldsymbol{\Delta}_{\alpha,\ell,t} - k h_s \boldsymbol{\Delta}_{\alpha,\ell,t} + \boldsymbol{g}$$

bending of the mean path is penalised –

the mean path is a smooth curve in space

$$F = \underbrace{\frac{k}{2}\sum_{a=1}^{f}\int_0^{N_a}\left[\left(\frac{\partial \bar{\boldsymbol{r}}_{\alpha,\ell}}{\partial \ell}\right)^2 + \boxed{\frac{1}{h_s}\left(\frac{\partial^2 \bar{\boldsymbol{r}}_{\alpha,\ell}}{\partial \ell^2}\right)^2}\right] d\ell}_{\text{mean path}} + \underbrace{\frac{k}{2}\sum_{a=1}^{f}\int_0^{N_a}\left[\left(\frac{\partial \boldsymbol{\Delta}_{\alpha,\ell,t}}{\partial \ell}\right)^2 + h_s\left(\boldsymbol{\Delta}_{\alpha,\ell,t}\right)^2\right] d\ell}_{\text{fluctuations}}$$

$$\mathbf{r}_{\alpha=1,\ell=0,t} = \mathbf{r}_{\alpha=2,\ell=0,t} = \ldots = \mathbf{r}_{\alpha=f,\ell=0,t} \tag{A1a}$$

$$\left.\frac{\partial \mathbf{r}}{\partial \ell}\right|_{\alpha=1,\ell=0} + \left.\frac{\partial \mathbf{r}}{\partial \ell}\right|_{\alpha=2,\ell=0} + \ldots + \left.\frac{\partial \mathbf{r}}{\partial \ell}\right|_{\alpha=f,\ell=0} = 0 \tag{A1b}$$

$$\left.\frac{\partial \mathbf{r}}{\partial \ell}\right|_{\alpha=1,\ell=N_a} = \left.\frac{\partial \mathbf{r}}{\partial \ell}\right|_{\alpha=2,\ell=N_a} = \ldots = \left.\frac{\partial \mathbf{r}}{\partial \ell}\right|_{\alpha=f,\ell=N_a} = 0 \tag{A1c}$$

$$\sum_{\alpha=1}^{f} s_{i\alpha} = 0$$

$$\sum_{\alpha=1}^{f} s_{i\alpha}^2 = f$$

$$\sum_{\alpha=1}^{f} s_{i\alpha} s_{j\alpha} = 0$$

Cosine modes on an arm   Xp→ N/p domains, length scales of sqrt(Nb2/p)

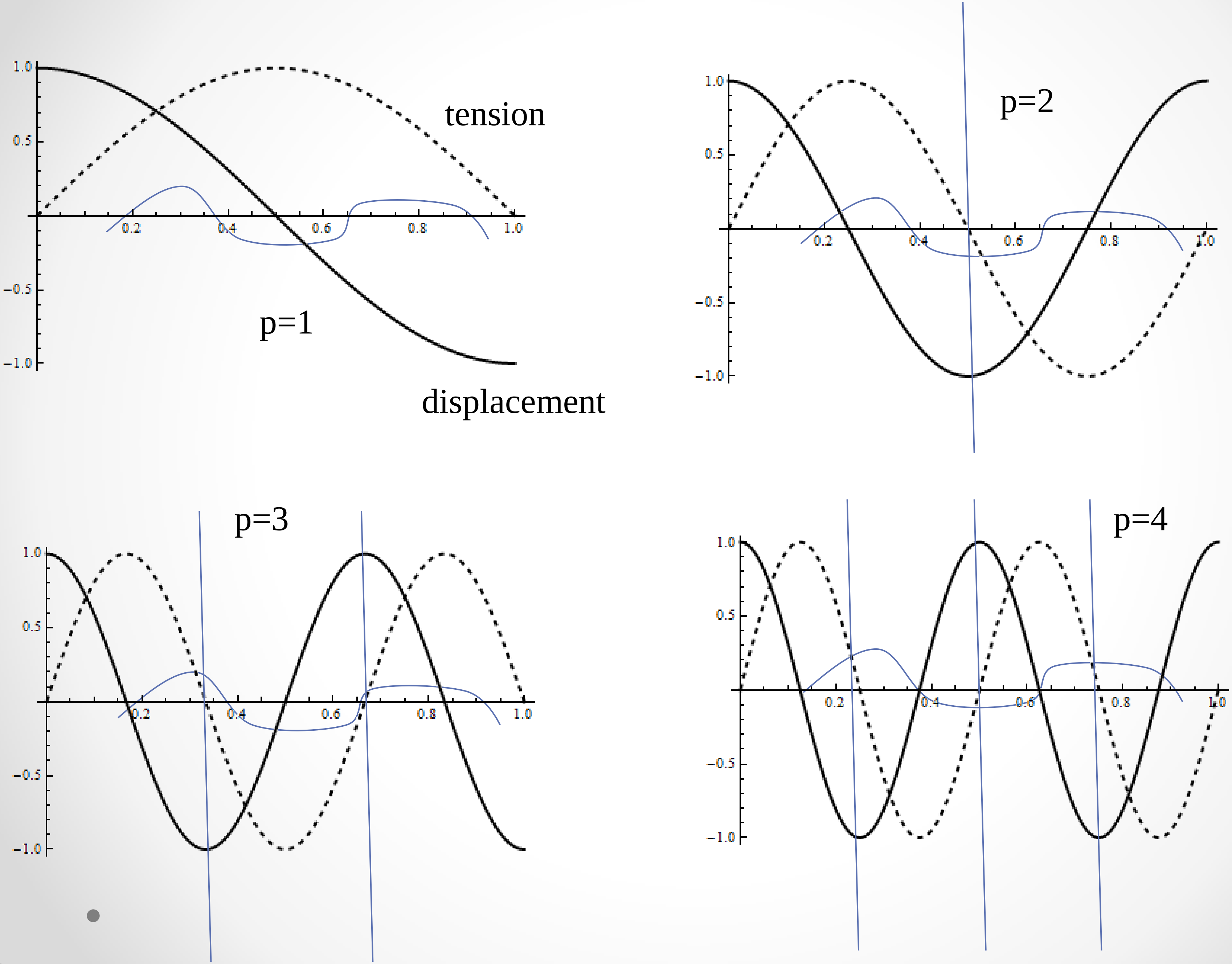

Xp→ N/p domains, length scales of sqrt(Nb2/p)

a cosine and a sine mode

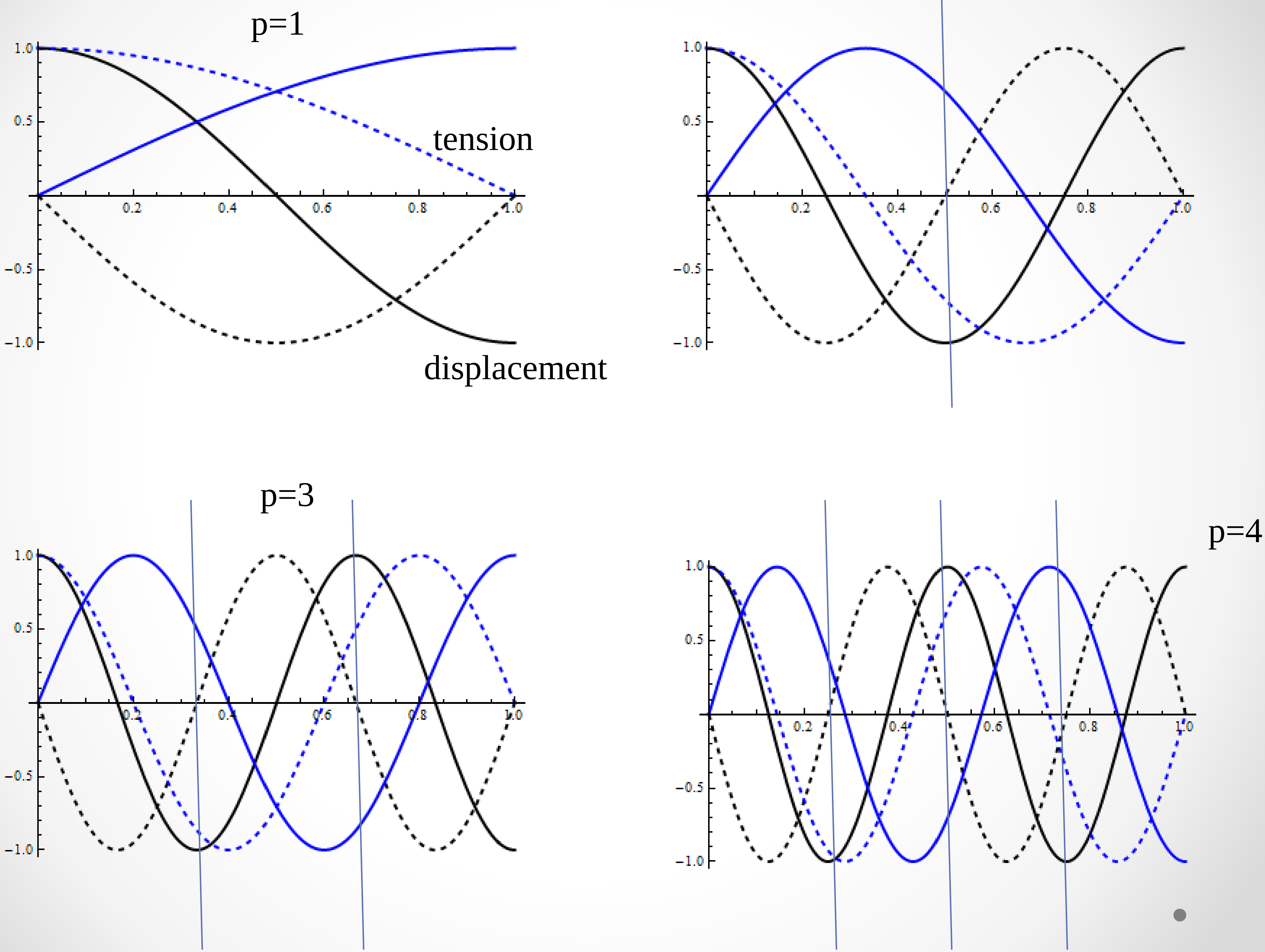

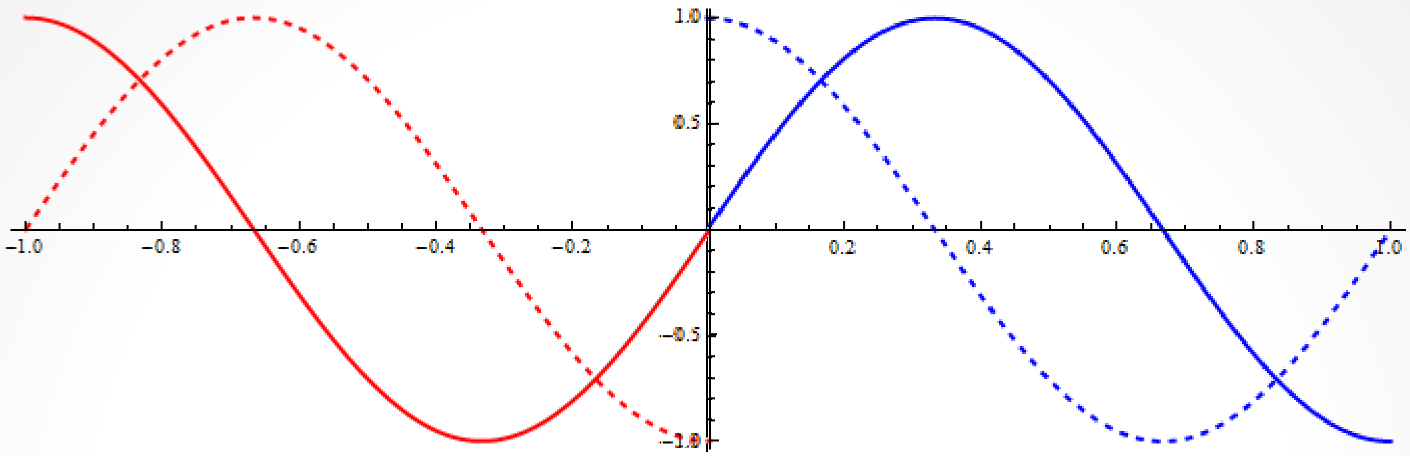
1.0
0.5
−0.5
−1.0
−1.0
−0.8
−0.6
−0.4
−0.2
0.2
0.4
0.6
0.8
1.0

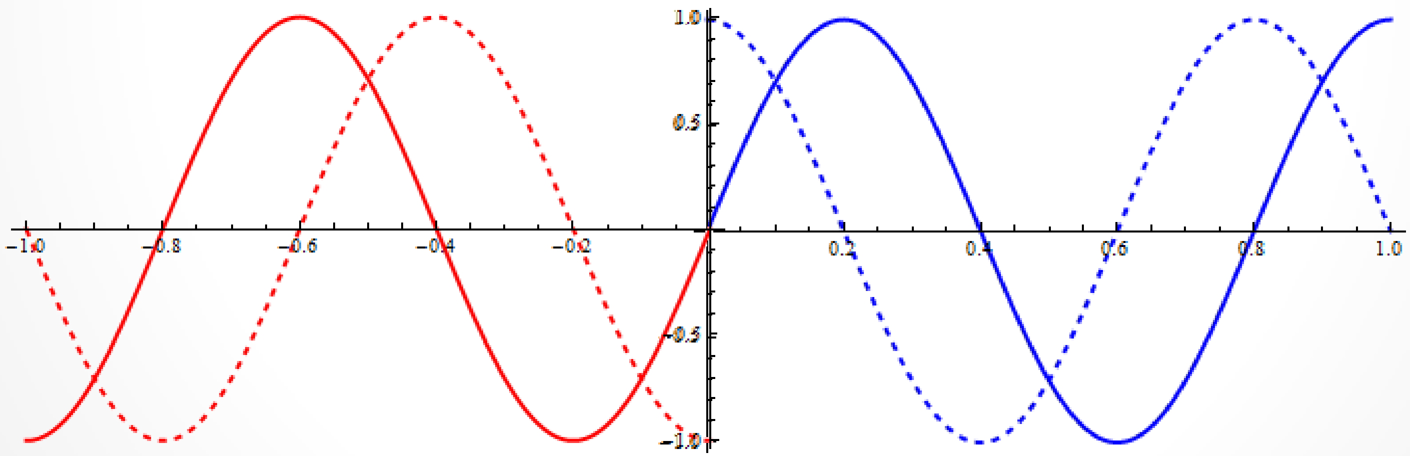
1.0
0.5
−0.5
−1.0
−1.0
−0.8
−0.6
−0.4
−0.2
0.2
0.4
0.6
0.8
1.0

Linear chain correlators

The correlator does not decay with internal Rouse modes for central segments

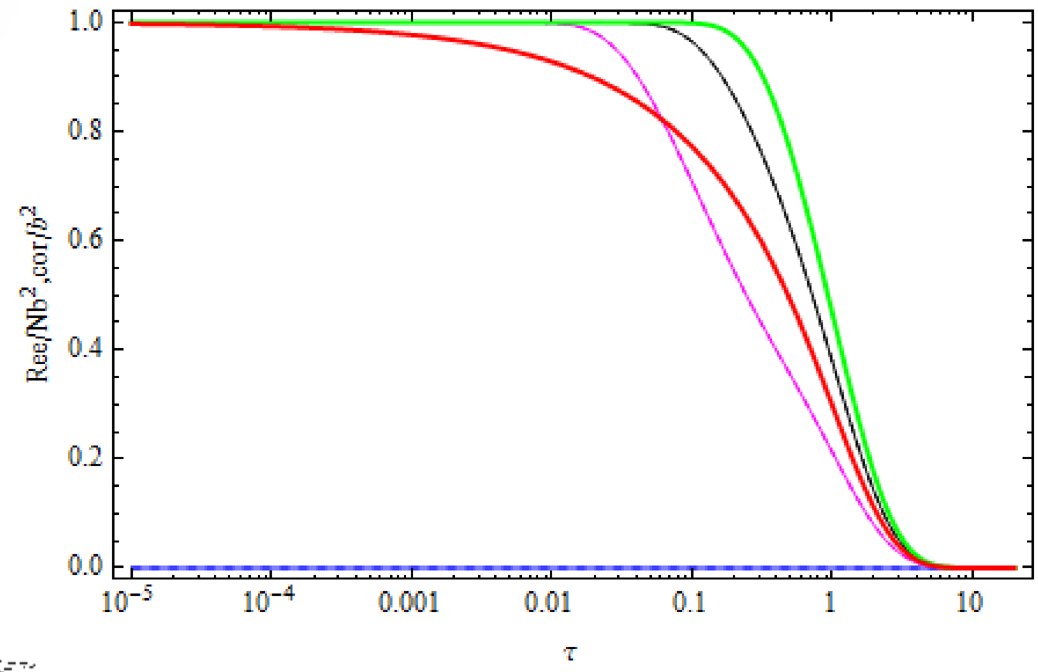

blue:ends
green: middle
red: 0.15/0.85
black: 0.3/0.7
magenta: *Ree*

Free ends 2 – Unentangled case/THEORY

Rouse modes only

***φ(t) from* MD 1**

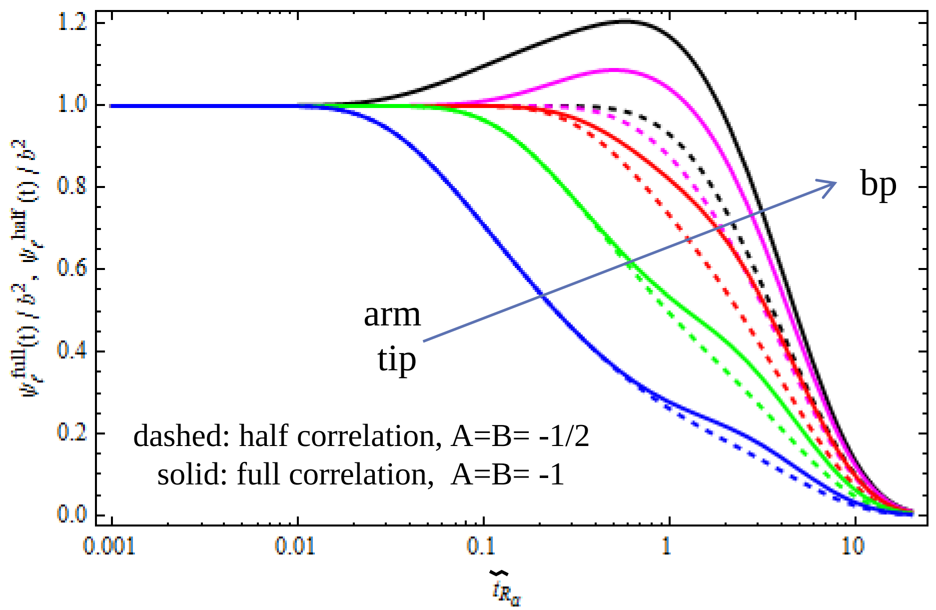

For the inner segments the correlator decays only at timescales of the order of $\tau_{R\alpha}$

The half correlation (A = B = -1/2) removes the undesirable peak

$$\psi_\ell(t) = < \boldsymbol{u}_{a,\ell,0} \cdot (\boldsymbol{R}_a - A\boldsymbol{R}_\beta - B\boldsymbol{R}_\gamma) >$$

Cayley tree

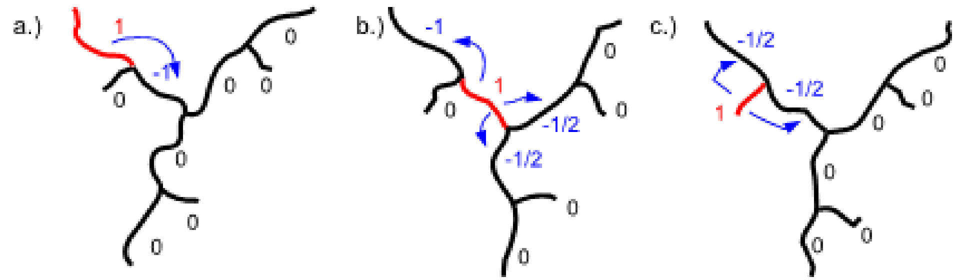

Symmetric star

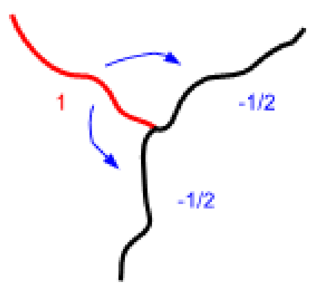

Mean-square internal distance $R^2(n)$

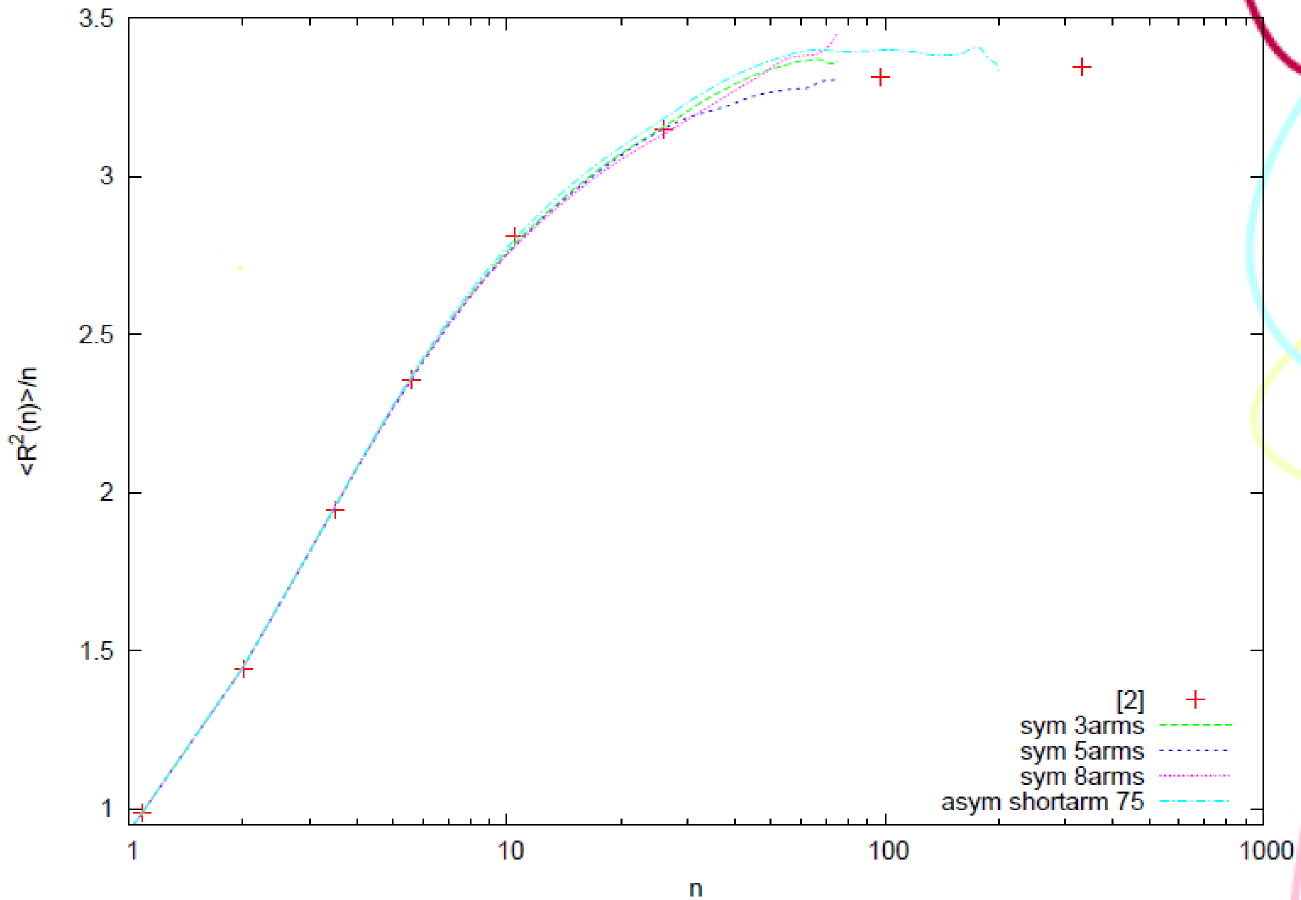

$b^2 = 3.4$ in simulation units

SIMULATION

Simulation details

System under investigation

Method

- Molecular dynamics
- Monte Carlo

Systems

- symmetric stars:
  N_a=3,5,8 L_a=75(Z=3)
- asymmetric stars:
  N_a=3 L_{a1}=200(Z=8)
  L_{a2}=75(Z=3),50(Z=2)

Details

- high T (far above T_g)
- time scale units $\approx$ 1 ps

Model

- bead-spring model, LJ + FENE
- semiflexible stars, $N_e \approx 25$

$$U_{bend}(\phi) = 2(1 - \cos \phi)$$

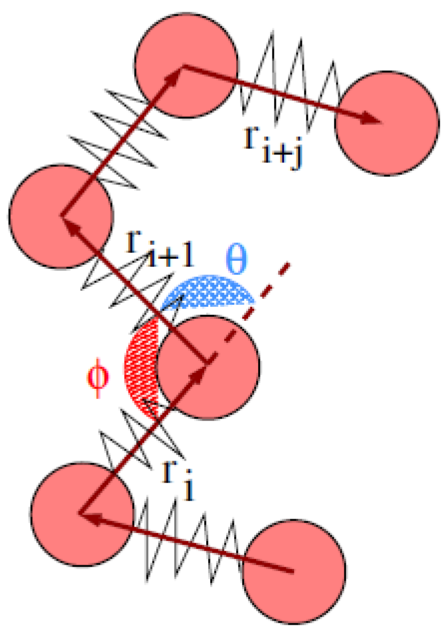

Bending Modes

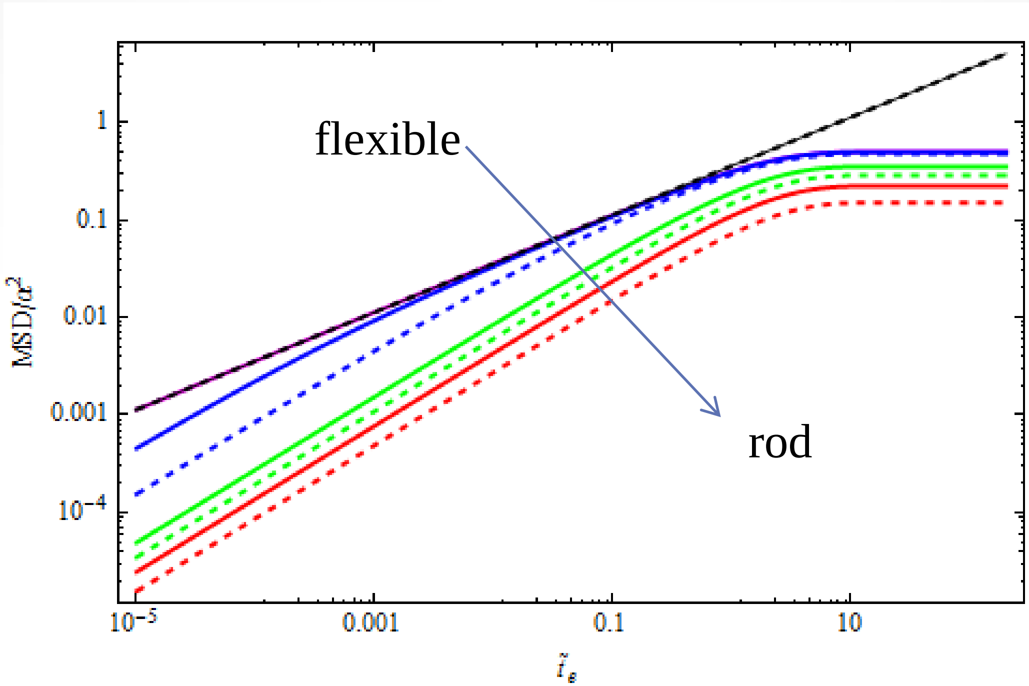

well entangled
chain

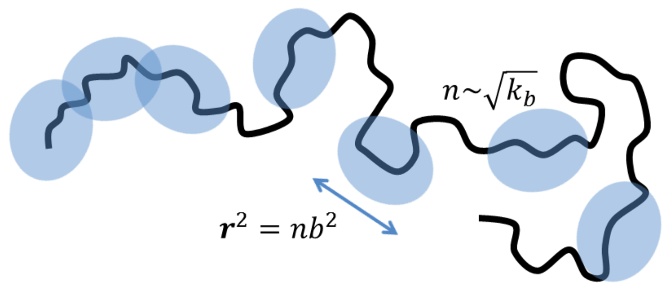

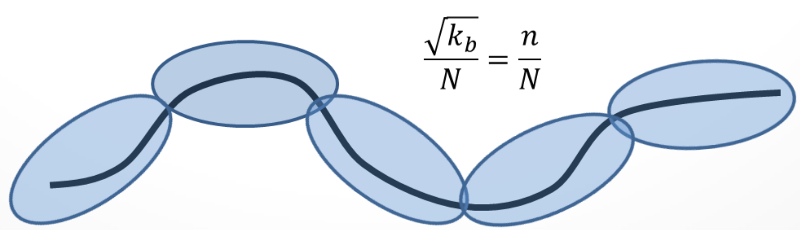

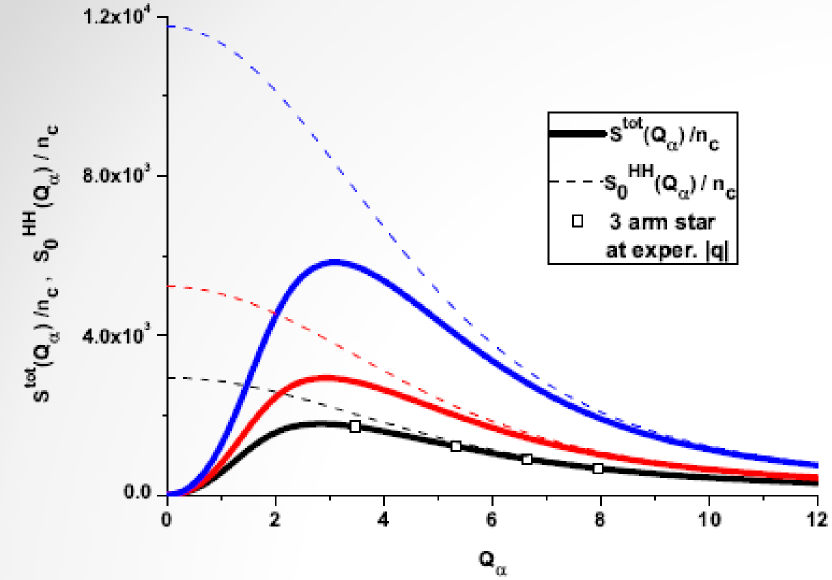

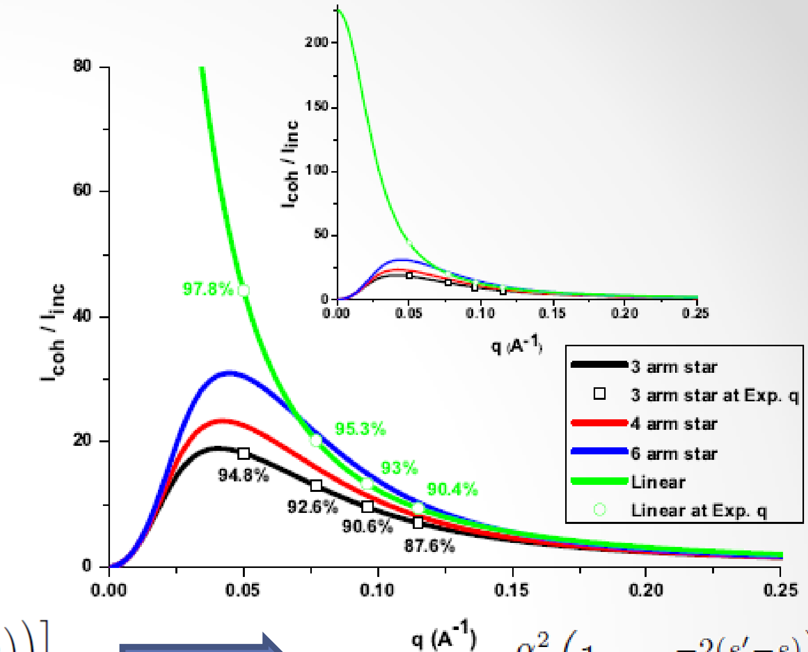

$$< MSD_{BV} >= \frac{\alpha^2}{2} - \frac{\alpha^2}{4}\left[e^{-2(s'-s)}\left(1-\Phi\left(\frac{2\sqrt{\tilde{\tau}}}{\pi}-\frac{\pi(s'-s)}{2\sqrt{\tilde{\tau}}}\right)\right)+e^{2(s'-s)}\left(1-\Phi\left(\frac{2\sqrt{\tilde{\tau}}}{\pi}+\frac{\pi(s'-s)}{2\sqrt{\tilde{\tau}}}\right)\right)\right]$$

$$\frac{\alpha^2}{2}\left(1-e^{-2(s'-s)}\right)$$